Ionoelectronics. Pillarlike Aggregates Formed via Highly Nonlinear Complexation Processes. A Light-Scattering Study

Thierry Toupance,[†] Henri Benoit,[‡] Dominique Sarazin,[‡] and Jacques Simon*[,†]

Contribution from ESPCI-CNRS, 10, rue Vauquelin 75231 Paris cedex 05, France, and ICS-CNRS, 6, Rue Boussingault 67083 Strasbourg Cedex, France

Received December 27, 1996[⊗]

Abstract: A bisphthalocyanine lutetium derivative substituted with benzo-15-crown-5 subunits, $[(15C5)_4Pc]_2Lu$ (**1**), has been shown to form sandwich complexes with cations such as potassium ion, the complexes further form pillarlike aggregates. Light scattering studies have been carried out as a function of the ratio $[K^+]/[\mathbf{1}]$ in order to determine the characteristics of the aggregates. It has been demonstrated that high molar mass aggregates ($\bar{M}_w$ about 10^6) are formed even at small $[K^+]/[\mathbf{1}]$ ratios, they coexist with uncomplexed monomeric $[(15C5)_4Pc]_2Lu$. The transformation from the metal-free monomer to the metal ion-containing aggregate involves a highly nonlinear two-stage complexation process. The shape of the aggregate is very probably rodlike (pillar-type structure) as indicated by the angle dependence of the light scattered.

Introduction

Ionoelectronics is defined as the domain of science which involves the storage and the processing of information using metallic or molecular ions as active species.[1,2] The treatment of information is always connected to various nonlinear effects. Indeed, linear or quasi-linear processes inevitably lead to a rapid randomization of the input signal during the processing. This necessity of nonlinearity, which is essential to having well-defined states, can be illustrated by the Conway's game of life.[3]

A surface is divided into two-dimensional (^{2}D) cells which can be either zero (white) or one (black). The input information is first transformed into a set of zero and one states and is introduced within the network formed by the ^{2}D cells by addressing some of the elementary cells (Figure 1).

In considering the case of the complexation of ions, the zero (off) or one (on) states may be defined as the free ligand and the corresponding metal complex, respectively.

The state of the unaddressed elementary cells is determined by considering the eight nearest neighbors; the switching rules are as follows:

(1) An elementary unit switches from "off" to "on" if three neighbors are themselves "on". Otherwise, it remains "off".

(2) An elementary unit remains "on" when two or three neighbors are "on". It turns "off" in the other cases.

These, evidently arbitrary, rules lead to a well-defined processing of the input signal. If the parallel with ion complexation is conserved, one can consider plugs (cells) functionalized with ion-complexing ligands; the complexation must be nonlinear and only pure complexes or free ligands are linked on each plug. The "off-to-on" transition induced by the input signal on one of the elementary cells will significantly reduce the concentration of cation within this cell. After some time, the nearest elementary cells will experience a cation concentration decrease due to ion diffusion, whereas the ligands, bound to the surface, cannot migrate. Depending on the threshold concentration necessary to switch the state, the neighboring cell will remain at its initial state or will switch. Ion diffusion therefore ensures the necessary interaction between the various contiguous elementary cells which is necessary to have an information treatment.

Information processing in the network is continued until a stable state is reached, if any[2,3] (Figure 1). The degree of interest of this system is entirely determined by the nonlinearity of the switching processes and by the rules chosen.

The key feature in the ionoelectronics system previously described is the use of a ligand able to yield a high positive cooperative complexation.

Helix−coil transitions of ionic polysaccharides[4,5] or polypeptides,[6,7] among other examples, involve highly cooperative processes. However, in most cases, the transition is more sensitive to temperature changes rather than to ion concentration differences.

Lutetium bisphthalocyanine substituted with crown-ether subunits has been designed and synthesized to afford nonlinear ion complexation processes (Figure 2).[2]

$[(15C5)_4Pc]_2Lu$ (**1**) in presence of large cations such as K^+ gives sandwich complexes which further yield cofacial aggregates via a highly cooperative complexation process. The nonlinear character was deduced from the slope of the titration curve $[\mathbf{1}]/[KSCN]$ determined by UV−visible spectroscopy.[2]

Previously, studies[8−12] on monophthalocyanine complexes $(15C5)_4PcM$ and $(18C6)_4PcM$ (M = H_2, Zn, Ni, Co, Cu, etc.) were carried out in a similar way. In the case of the 15-crown-5 copper derivative, the $[(15C5)_4PcCu]$ vs [KCl] plot gives the indication that the dimeric sandwich complex is formed via a nonlinear process. This hypothesis was not however evoked

[†] ESPCI-CNRS.

[‡] ICS-CNRS.

[⊗] Abstract published in *Advance ACS Abstracts,* September 1, 1997.

(1) Simon, J.; Engel, M. K.; Soulié, C. *New J. Chem.* **1992**, *16*, 287.

(2) Toupance, T.; Ahsen, V.; Simon, J. *J. Am. Chem. Soc.* **1994**, *116*, 5352; *J. Chem. Soc., Chem. Commun.* **1994**, 75.

(3) Weisbuch, G. In *Dynamique des systèmes complexes* (*Dynamics of Complex Systems*); Inter Editions/Editions du CNRS, Paris, 1989.

(4) Nilsson, S.; Piculell, L. *Macromolecules* **1990**, *23*, 2776.

(5) Rochas, C.; Rinaudo, M. *Biopolymers* **1984**, *23*, 735.

(6) Doty, P.; Yang, J. T. *J. Am. Chem. Soc.* **1956**, *78*, 408.

(7) Zimm, B. H.; Bragg, J. K. *J. Chem. Phys.* **1959**, *31*, 526.

(8) Kobayashi, N.; Lever, A. B. P. *J. Am. Chem. Soc.* **1987**, *109*, 7433.

(9) Sielcken, Ot. E.; van Tilborg, M. M.; Roks, M. F. M.; Hendriks, R.; Drenth, W.; Nolte, R. J. M. *J. Am. Chem. Soc.* **1987**, *109*, 4261.

(10) Ahsen, V.; Yilmazer, E.; Ertas, M.; Bekâroğlu, O. *J. Chem. Soc., Dalton Trans.* **1988**, 401.

(11) Gasyna, Z.; Kobayashi, N.; Stillman, M. J. *J. Chem. Soc., Dalton Trans.* **1989**, 2397.

(12) Kobayashi, N.; Togashi, M.; Osa, T.; Ishii, K.; Yamaushi, S.; Hino, H. *J. Am. Chem. Soc.* **1996**, *118*, 1073.

S0002-7863(96)04443-5 CCC: $14.00

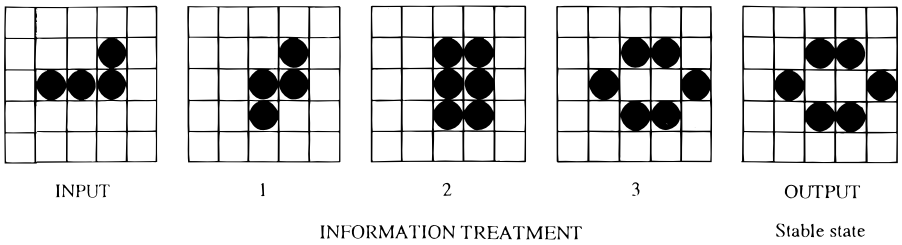

Figure 1. Conway's game of life. The "on" (or one) and "off" (or zero) states are schematized by the black and white colors, respectively. Input and output informations are represented on the left and right sides, respectively. Three "generations" of information processing are represented.

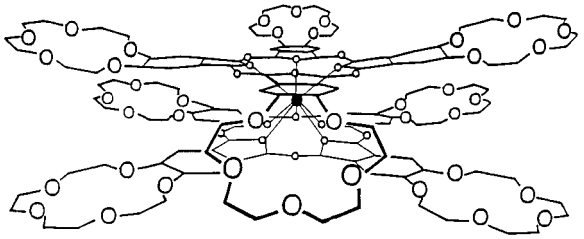

Figure 2. The lutetium bisphthalocyanine derivative substituted with 15-crown-5 subunits synthesized: $[(15C5)_4Pc]_2Lu$, **1** (after ref 2).

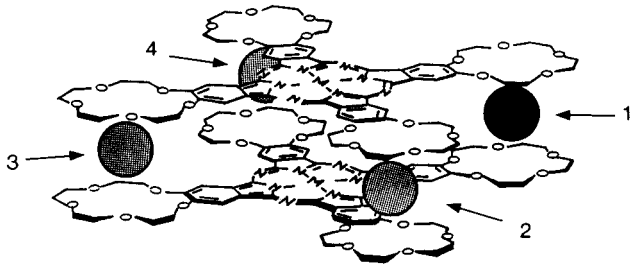

Figure 3. Representation of the dimeric sandwich complex formed from monophthalocyanine derivatives $(15C5)_4PcM$ (from refs 2 and 8).

at that time.[9] The relationship between the shape of the titration curve and the nonlinearity was clearly demonstrated later on[2] with the lutetium derivative **1**. It was then postulated that the first cation is difficult to complex, whereas the second, the third, and the fourth ones are more easily bound (see Figure 3):

$$K_4, K_3, K_2 > K_1$$

By using lutetium bisphthalocyanine derivatives, the ion complexation does not stop at the dimeric stage and aggregates can be formed. It is demonstrated by light-scattering measurements in the present article that the addition of KSCN to $[(15C5)_4Pc]_2Lu$ affords high molar mass aggregates via two successive highly nonlinear processes. This results in the coexistence of large aggregates with uncomplexed monomeric ligand **1**. The origin of these nonlinear effects is discussed in detail in the following sections.

Light-Scattering Measurements

(a) Characterization of the Formation of Aggregates. When light goes through a solution containing particles, scattering occurs. Its intensity strongly depends on the size of the particles. Particles smaller than $\lambda/20$ (λ, wavelength of the electromagnetic wave), which corresponds in the visible range to approximately 200−300 Å, may be considered as points and will scatter light as such. Particles of sizes larger than $\lambda/20$ lead to more important light scattering with a large angular dependence (θ) (see below) whereas this angular dependency does not significantly occur for smaller particles.[13]

The amount of scattered light is defined by the Rayleigh ratio R_θ (in cm^{-1}):

$$R_\theta = \frac{I_\theta}{Ve_o(1 + \cos^2\theta)}$$

where I_θ is the light scattered at the angle θ from the incident beam, V is the diffusing volume, and $e_o = I_o\, d\Omega/S$ ($d\Omega$, solid angle; S, surface irradiated; I_o, intensity of incident light).

R_θ is usually measured relatively to a reference substance (like benzene):

$$R_\theta = I_\theta(R_B^{90}/I_B^{90})$$

where R_B^{90} is the Rayleigh ratio at 90° for benzene and I_B^{90} is the corresponding intensity of scattered light.

For an incident radiation polarized perpendicular to the plane containing θ (see for instance refs 14 and 23):

$$\frac{K_v c}{\Delta R_\theta} = \frac{1}{\bar{M}_w P(\theta)} + 2A_2 c + ...$$

with $\Delta R_\theta = (R_\theta)_{solution} - (R_\theta)_{solvent}$ and $\bar{M}_w$ being the weight average molar mass of the diffusing particles of concentration c (in g cm^{-3}), $P(\theta)$, the function depending on the shape of the particles (structure factor) and A_2, the second virial coefficient (in mol cm^3 g^{-2}).

The constant K_v is related to the refractive index increment (dn/dc), the wavelength of the incident light (λ), the Avogadro's number N, and the refractive index of the solution n:

$$K_v = \frac{4\pi^2}{N\lambda^4} n^2 \left(\frac{dn}{dc}\right)^2$$

where K_v is in mol cm^2 g^{-2}.

In most cases the following variable is used instead of θ:

$$q = |\mathbf{q}| = \frac{4\pi n}{\lambda} \sin\frac{\theta}{2}$$

By definition the limit of the function $P(\theta)$ is one when $\theta \rightarrow 0$. If $1/\bar{M}_w \gg 2A_2c$ (A_2 is in general of the order of 10^{-4} mol cm^3 g^{-2}), ΔR_θ at small angles is proportional to the concentration of scattering particles:

$$(\Delta R_\theta)_{\theta\rightarrow 0} = \bar{M}_w K_v c$$

The difference of intensity ΔI_θ, which is directly related to ΔR_θ, as a function of the ratio $r = [KSCN]/[\mathbf{1}]$ with a constant lutetium derivative concentration (10^{-5} M) has been determined (Figure 4).

(13) Champetier, G.; Monnerie, L. In *Introduction à la Chimie Macromoléculaire (Introduction to Macromolecular Chemistry)*; Masson: Paris, 1969.

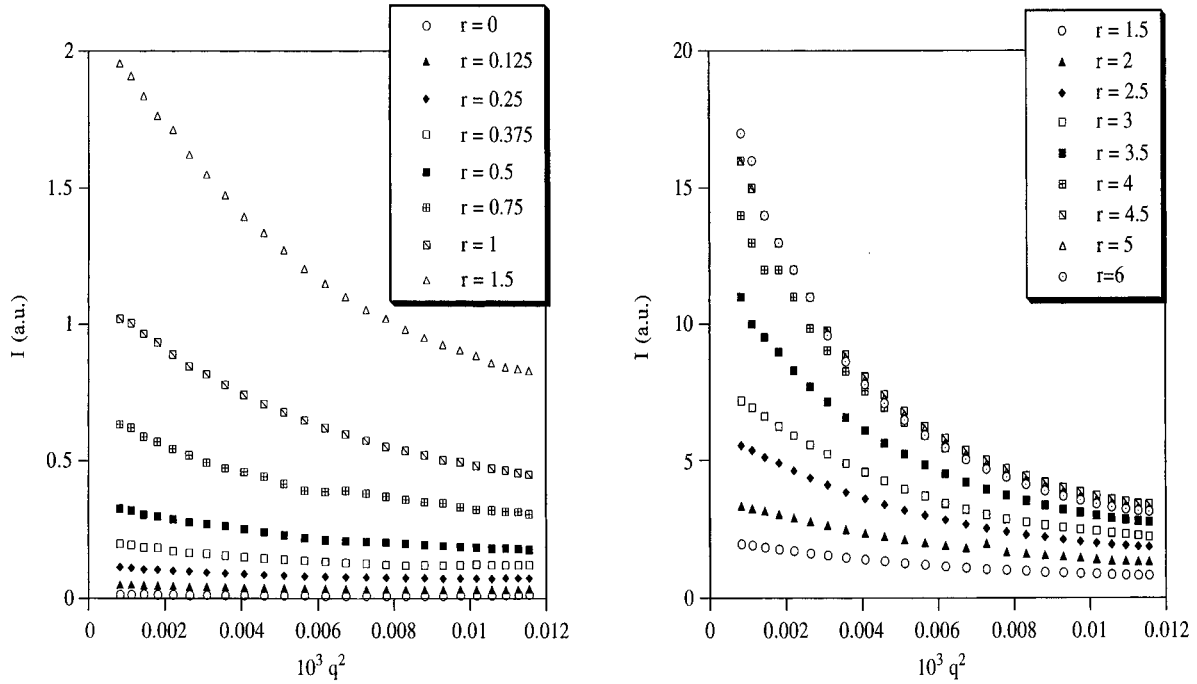

Figure 4. Intensity of scattered light (I_θ) (in arbitrary units) as a function of the ratio r = [KSCN]/[**1**] (solvent, $CHCl_3$; KSCN, 2×10^{-3} M in MeOH; [**1**] = 10^{-5} M) (q in Å^{-1}).

Pure chloroform leads, as expected, to a nearly angle-independent light scattering. The addition of KSCN in methanol to $CHCl_3$, in the concentration range used in further experiments, did not change the scattering intensity. In the case of pure $[(15C5)_4Pc]_2Lu$ (10^{-5} M) in $CHCl_3$, a slightly angle-dependent scattering could be detected but the absolute intensity was lower than the one of the pure solvent. Pure $CHCl_3$ and **1** in $CHCl_3$ lead to approximately the same curve after correction for the absorption of scattered light by the lutetium derivative. In contrast, the addition of KSCN to a chloroformic solution of $[(15C5)_4Pc]_2Lu$ affords a drastic enhancement of the scattered light with an important angular dependence (Figure 4). This clearly indicates the appearance of species whose size is larger than 200−300 Å.

It is possible, from UV−visible spectra, to measure the disappearance of the monomeric species as a function of the cation/lutetium derivative ratio.[2] A comparison with the appearance of the scattering species can then be made (Figure 5).

The disappearance of the monomeric form of $[(15C5)_4Pc]_2Lu$, when KSCN is added, follows approximately a straight line from r = [KSCN]/[**1**] = 0 to r = 4 to reach a plateau value. The corresponding slope is therefore related to a ratio of four potassium ions per one lutetium derivative. This is already an indication of the formation of aggregates which follows a nonlinear complexation process, since the ratio 4:1 can only be obtained for fairly large molar mass aggregates.[2]

Light-scattering measurements confirm that the aggregates have large sizes. Indeed, at the concentration of lutetium derivative considered (10^{-5} M), only large particles can be detected. Above a ratio of approximately two KSCN per lutetium derivative, the proportion of monomer which disappears is strictly equal to the amount of high molar mass aggregates which forms. In other words, by addition of a small quantity of cation, the uncomplexed monomeric lutetium derivative is integrally transformed into large-size aggregates with no noticeable formation of dimers, trimers, or other related oligomers which do not have sizes large enough to yield a significant scattering of light.

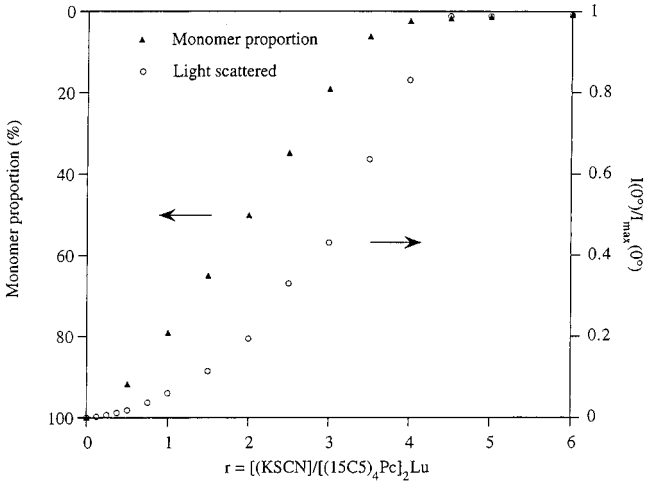

Figure 5. Disappearance of the monomeric form of $[(15C5)_4Pc]_2Lu$ as evidenced by optical spectra and light scattering (extrapolated at zero angle) for the same solutions ($CHCl_3$ 10^{-5} M) as a function of the ratio [KSCN]/[**1**]. Monomer proportion = [monomer]/[L_o]; L_o: initial ligand concentration.

Aggregates form up to a ratio four K^+ per one ligand: this behavior follows the one observed for the disappearance of monomeric $[(15C5)_4Pc]_2Lu$.

(b) Determination of the Molar Mass of the Aggregates. By plotting K_vc/I as a function of q^2 (c, concentration of aggregates derived from UV−visible measurements) it is possible to determine $1/\bar{M}_w$ by extrapolation to $\theta = 0$. The calculation of $\bar{M}_w$ necessitates the knowledge of the increment index (dn/dc). This value is around 0.2 cm^3 g^{-1} for conventional polymer/solvent couples such as polystyrene in tetrahydrofuran.[14] Its determination, using two different refractometers, led in our case to a significantly higher value (Table 1).

The refractive index increment found is of the order of 2.5 ± 0.8 cm^3 g^{-1}; this is unusually large probably because of the proximity of the absorption band. The fairly high uncertainty

(14) Brandrup, J.; Immergut, E. H. In *Polymer Handbook*; J. Wiley & Sons, New York, 1989.

Table 1. Refractive Index Increment of $[(15C5)_4Pc]_2Lu$

reference cell	measurement cell	d*n*/d*c*, cm^3 g^{-1}
$CHCl_3$[a] (2% MeOH)	$CHCl_3$ (2% MeOH) $[(15C5)_4Pc]_2Lu$ (10^{-5} M)	2.0
$CHCl_3$[a] (2.25% MeOH)	$CHCl_3$ (2.25% MeOH) $[(15C5)_4Pc]_2Lu$ (10^{-5} M) KSCN 4 10^{-5} M	2.2
$CHCl_3$[b] (2.25% MeOH)	$CHCl_3$ (2.25% MeOH) $[(15C5)_4Pc]_2Lu$ (10^{-5} M) KSCN 4 10^{-5} M	3.3

[a] Brice Phoenix differential refractometer (green light, $\lambda = 546$ nm). [b] CRM home-made differential refractometer (ANVAR patent) (white light).

Table 2. Weight Average Molar Mass of Aggregates Formed in Chloroformic Solutions $[(15C5)_4Pc]_2Lu$ in Presence of Different Amounts of KSCN[a]

r	$10^{-5}\,\bar{M}_w$, g mol^{-1}	$\bar{n}$	*r*	$10^{-5}\,\bar{M}_w$, g mol^{-1}	$\bar{n}$
0	not detect.	−	3.5	6.1	195
0.5	1.9	60	4	8.1	260
1	2.4	75	4.5	9.1	290
1.5	2.7	85	5	9.7	310
2	3.3	105	6	10	320
2.5	4.3	140	7	8.9	285
3	4.5	145			

[a] r = [salt]/[**1**]; $\bar{n} = \bar{M}_w/M$, M, molar mass of $[(15C5)_4Pc]_2Lu{\cdot}4$ KSCN.

is due to the low concentrations of **1** used (10^{-5} M). The refractive index increment does not seem to be affected by the addition of KSCN: the aggregated and monomeric forms of $[(15C5)_4Pc]_2Lu$ yield approximately the same result.

The weight average molar mass of the aggregates can now be calculated from the curves K_vc/I vs q^2 when q(or θ) $\rightarrow 0$ ($P(\theta) \rightarrow 1$) (Table 2). In further calculations, the (d*n*/d*c*) value will be taken as equal to 3 cm^3 g^{-1}.

In the previous calculations, no hypothesis concerning the shape of the aggregate has to be postulated. As previously expected, the molar mass of the scattering species formed by addition of KSCN is large, more than 10^5 g mol^{-1}; this corresponds to 60 molecular units. UV−visible measurements indicate a degree of aggregation greater than 20 is needed in order to be able to observe the stoichiometry four cations per one lutetium derivative.[2] Light-scattering determinations therefore show that this is indeed the case.

When the amount of KSCN increases, the average aggregation number increases, from 60 ($r = 0.5$) to 260 ($r = 4$). This approximate 4-fold increase is significant but not very large: a fairly narrow distribution of the molar mass of the aggregates is therefore probable. This point is discussed in the next section.

(c) Polymolecularity of the Aggregates. The light-scattering technique used as shown above leads to the following average molar masses:

$$\bar{M} = \frac{\sum_i n_i M_i^p}{\sum_i n_i M_i^{p-1}}$$

where n_i and M_i are number and mass of the species i, respectively, and for $p = 1$, $\bar{M} = \bar{M}_n$ (number average molar mass), for $p = 2$, $\bar{M} = \bar{M}_w$ (weight average molar mass), and for $p = 3$, $\bar{M} = \bar{M}_z$ (z average molar mass).

The summation is extended to all the species in the solution provided they have the same refractive index increment.

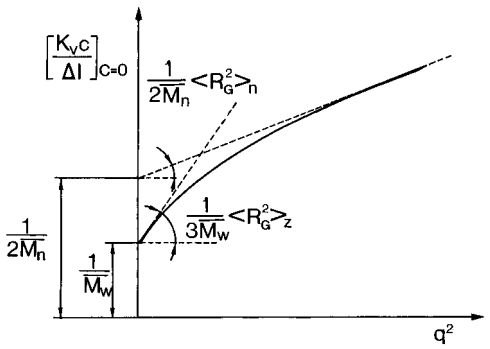

Figure 6. Various parameters which can be derived from the $K_vc/\Delta I$ vs q^2 curve: $\langle R_G^2\rangle_z$, z average of the square of the radius of gyration R_G; $\langle R_G^2\rangle_n$ n average of R_G^2.

The weight average $\bar{M}_w$ and number average $\bar{M}_n$ molar masses can be both measured by light scattering. The polymolecularity, P, of the system is given by the ratio

$$P = \bar{M}_w/\bar{M}_n$$

The examination of the angular dependence of the scattered light allows the determination of the polymolecularity since, as previously mentioned, the largest particles contribute more to the scattering at large angles than at small angles. A quantitative estimate of the polymolecularity can be made for Gaussian polymeric chains.[15] The extrapolation to $\theta = 0$ gives the value of $1/\bar{M}_w$ whereas the extrapolation of the curve arising from the large angle region ($\theta \rightarrow 180°$) affords $1/2\bar{M}_n$ (Figure 6).

This method of determination of the polymolecularity is satisfactory even for other shapes of molecules or aggregates whenever high molar masses are considered.

The experimental results for $[(15C5)_4Pc]_2Lu$ in $CHCl_3$ as a function of various concentrations of KSCN are shown in Figure 7.

Whatever the ratio r = [KSCN]/[**1**], the curves K_vc/I vs q^2 are approximately linear. This indicates that the polymolecularity, P, is of the order of 2. This means that for an aggregate with $\bar{M}_n = 10^6$, there is a factor of approximately 10 between the 10% smallest and 10% largest aggregates. The polymolecularity does not seem to be largely influenced by the cation to lutetium derivative ratio. It is noteworthy that statistical polymerization leads also to a polymolecularity of about two.

(d) Shape of the Aggregate. The function $P(q)$ is dependent upon the structural model used for the scattering particles.

Because of the very nature of the complexation processes which lead to the aggregates, a pillarlike structure seems highly probable. The UV−visible measurements are consistent with this hypothesis. A schematic representation of such an aggregate has been featured in Figure 8.

The theoretical curve of $P(ql)$ for rodlike diffusing particles (where l is the length of the rod) is known[13] and the experimental results can be compared to theoretical models. In the two cases represented (Figure 9a,b), the length of the rodlike particles has been allowed to vary for all the stoichiometries ratios r studied ($r = 0-6$) (model 1).

The experimental results have been treated as follows. For small KSCN concentrations ($0 < r \leq 0.5$), the experimental points can be well fitted to the theoretical equation corresponding to rodlike particles. The experimental points obtained for higher r ratios can then be fitted to the same curve by adjusting l_2 (the length of the rod) considered as a parameter. The

(15) Benoit, H. *J. Polym. Sci.* **1953**, *11*, 507.

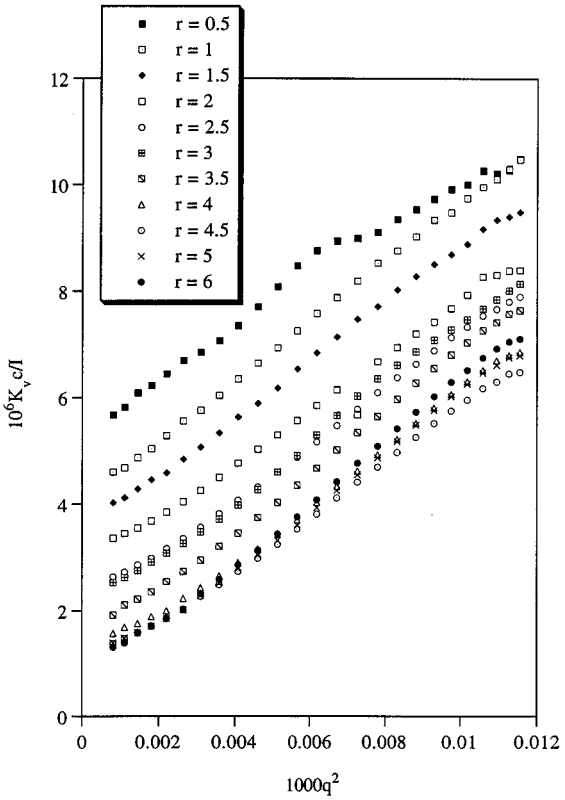

Figure 7. Light scattered expressed as $K_v c/I$ as a function of q^2. c is the concentration of aggregates (in g cm^{-3}) determined from UV−visible spectra (q in Å^{-1}).

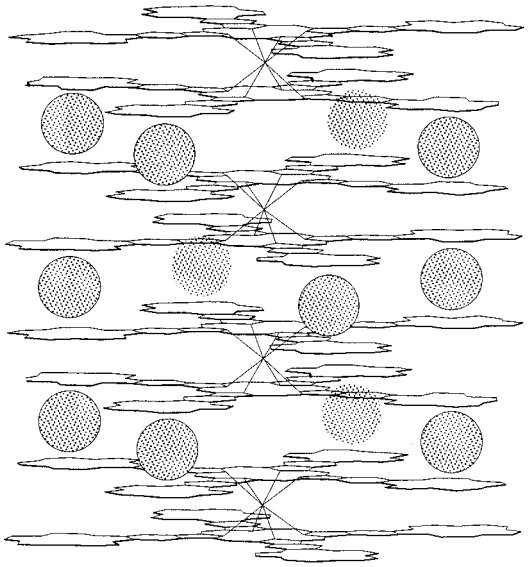

Figure 8. Pillarlike structure postulated for the aggregates formed by complexation of the potassium ion with $[(15C5)_4Pc]_2Lu$.

agreement between the experimental (Figure 9a) and theoretical (Figure 9c) curves is poor at large angles; it can be improved if one takes into account the diameter of the rod (taken to be equal to 30 Å according to CPK models).

The z average radius of gyration of the particle $\langle R_G^2\rangle_z$ may be on the other hand deduced from the slope near zero angle of the curve $K_v c/I$ vs q^2 as shown on Figure 6. By plotting l_2^2 vs $\langle R_G^2\rangle_z$ a straight line is found with a slope very close to the theoretical value: $^1/_{13}$ instead of $^1/_{12}$. A quantitative comparison can now be made between $\langle R_G^2\rangle_z$ and the corresponding rod length l_2 deduced from $P^{-1}(ql)$ vs (ql) curves (Figure 9) (Table 3).

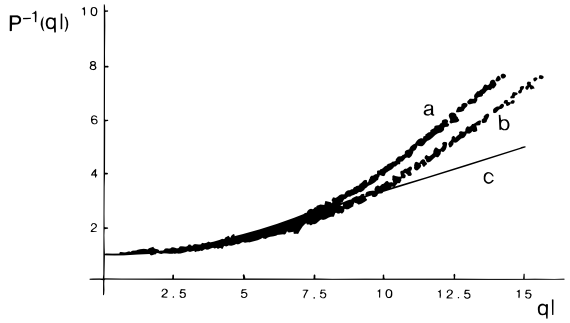

Figure 9. The curves $P^{-1}(ql)$ vs (ql) for (a) experimental points (l has been adjusted for all experimental points at stoichiometric ratios between 0 and 6, considering rodlike particles). (b) same as in curve a taking into account the diameter of the aggregate (30 Å), and (c) theoretical curve for a simple rodlike particle with no adjustment of l.

Table 3. The z Average of the Radius of Gyration R_G and the Experimental Rod Lengths l_1 and l_2 Determined As Indicated in the Caption for the Couple $[(15C5)_4Pc]_2Lu$/KSCN (distances in Å)

r	$\langle R_G^2\rangle_z^{1/2}$ [a]	l_1 [b]	l_2 [c]	r	$\langle R_G^2\rangle_z^{1/2}$ [a]	l_1 [b]	l_2 [c]
0.5	540	1 850	1 850	3.5	880	3 050	3 250
1	620	2 150	2 200	4	970	3 350	3 550
1.5	610	2 100	2 300	4.5	1 020	3 550	3 700
2	610	2 100	2 400	5	1 070	3 700	3 900
2.5	720	2 500	2 700	6	1 150	4 000	4 100
3	750	2 600	2 850	7	1 180	4 100	4 200

[a] Determined from Zimm's plots. [b] Calculated from $\langle R_G^2\rangle_z = l^2_1/12$ (pure rodlike model). [c] Calculated from $P^{-1}(ql)$ vs (ql).

The rod lengths calculated from the shape factor $P(ql)$, (l_2), or from the slope of the curve $K_v c/I$ vs q^2, (l_1), are in good agreement for all cation to lutetium derivative ratios. It is worth noting that the way of averaging l_1 and l_2 is not identical. This does not preclude a satisfactory agreement between them. EPR (electron paramagnetic resonance) studies on $[(15C5)_4Pc]_2Lu$ in $CHCl_3$ in presence of potassium picrate[16] allowed us to calculate the distance between two consecutive molecular units within the aggregate: a value around 8.8 Å has been found. The same value has been measured on a related molecular system.[17] The knowledge of this distance permits the calculation of the molar mass of the aggregate from the previously determined lengths of the rods. At $r = 0.5$, a molar mass around 6×10^5 is found; it increases up to 1.5×10^6 at $r = 7$. These values are in remarkable agreement with the ones determined from Zimm's plots (Table 2).

A more general model in which elementary rods are linked to each others in a statistical way via joints can be alternatively postulated (model 2). This model is derived from a previously described one[22] in which an alternating block copolymer made of rods and Gaussian chains is considered. As previously shown, the experimental points are fitted to the theoretical curve by varying l_c which is, this time, the length of the elementary rods linked to each others to form the overall aggregate. Meanwhile, the number of joints is considered to be constant. The best results of various fits have been represented on Figure 10.

It can be seen from Figure 10 that there is a good agreement between the experimental points and the theoretical curve with 25 elementary rods linked by joints (other number of rods gives a poorer fit). It is then possible to calculate the corresponding molar mass by taking the intermolecular distance of 8.8 Å within the aggregate as previously mentioned. The values calculated in this way are shown in Table 4.

(16) Toupance, T. Thèse de doctorat, Paris, 1995.
(17) Ishikawa, N.; Kaizu, Y. *Chem. Phys. Lett.* **1993**, *203*, 472.

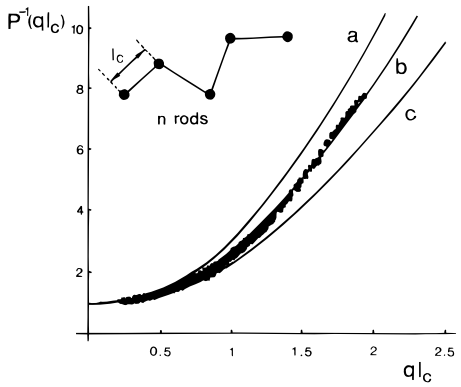

Figure 10. Theoretical curves for the plot $P^{-1}(ql_c)$ versus (ql_c) (l_c, length of the elementary rod; n, number of rods): a, $n = 30$; b, $n = 25$; c, $n = 20$. The experimental points are figured as squares (model 2).

Table 4. Values of the Length of the Elementary Rods (l_c) as a Function of the Ratio [KSCN]/[**1**] Postulating a Model in Which 25 Rods Are Linked by Joints[a]

r	l_c	$(M)_{ap} \times 10^{-5}$, g mol^{-1}	r	l_c	$(M)_{ap} \times 10^{-5}$, g mol^{-1}
0.5	260	23	3	380	33
1	280	25	4	480	42
1.5	300	26	6	550	48
2	310	27	7	570	50
2.5	365	32			

[a] Molar mass of 4 KSCN·[(15C5)$_4$Pc]$_2$Lu = 3 109, l_c is given in Å. $(M)_{ap}$: apparent molar mass.

The fitted elementary rod length l_c, varies from 260 to 570 Å depending on the amount of KSCN added. In the same time, the molar mass of the aggregates increases from 2.3×10^6 g mol^{-1} for $r = 0.5$ to 5×10^6 g mol^{-1} for $r = 7$. These values are approximately from 5 to 10 times higher than the ones deduced from Zimm's plots by extrapolating to $\theta = 0$ the $K_v c/I$ vs q^2 curves. This can be due to the uncertainty associated with the determination of (dn/dc) which intervenes as a square in the expression of the molar mass.

As a matter of fact, a change in (dn/dc) affects the value of the weight average molecular weight obtained by plotting $K_v c/I$ vs q^2 for $\theta \rightarrow 0$. The other determinations l_1, l_2, and l_c do not depend on dn/dc. In consequence, a change of dn/dc could give a better agreement with model 2 instead of model 1 as it is presently the case.

Mechanisms Involved in the Nonlinear Complexation

In order to rationalize the various results, it was important to demonstrate the reversibility of the formation of aggregates. The cryptand [2.2.2][18] is a tricyclic ligand which is known to selectively complex the potassium ion with a stability constant several orders of magnitude higher than the benzo-15-crown-5 derivatives. The addition of [2.2.2] to a solution of [(15C5)$_4$-Pc]$_2$Lu·4KPic (Pic, picrate ion) restores the initial light absorption spectrum whenever the concentration of [2.2.2] is equal to the one of K^+ (Figure 11).

The addition of [2.2.2] to the potassium complex aggregates (so-called reverse direction of the titration) is also characterized by a slope corresponding to four cations per lutetium derivative. The cation-induced aggregation process is therefore perfectly reversible. Nonselective aggregation phenomena can be excluded. The value of the slope (4:1) is an indication that the fourth stability constant (see Figure 3) is significantly larger than the other ones:

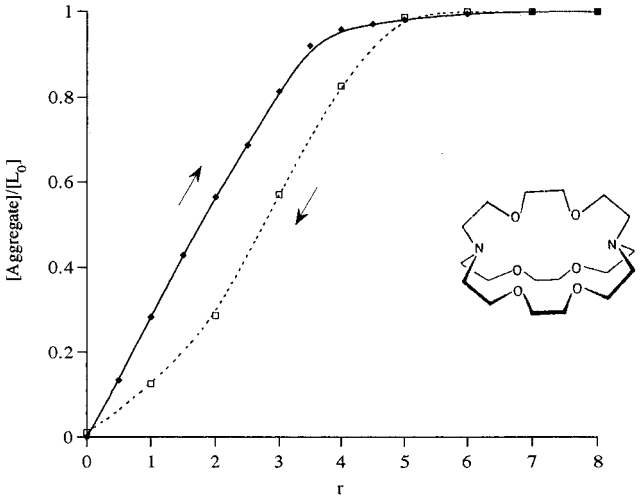

Figure 11. Concentration of aggregates versus the ratio $r = [K^+]/[L_o]$ (direct direction) or $r = 8\ (1 - [2.2.2]/[K^+])$ (reverse direction) (8 is the total number of added potassium ion): $[L_o] = [(15C5)_4Pc]_2Lu = 10^{-5}$ M in $CHCl_3$; $[K^+$ picrate$] = 2 \times 10^{-3}$ M in MeOH; and [2.2.2] $= 2 \times 10^{-3}$ M in $CHCl_3$.

$$K_4 \gg K_3; K_2 > K_1$$

Deaggregation must indeed start by the decomplexation of the fourth cation: it seems that whenever this is achieved, the aggregate made of n lutetium bisphthalocyanine molecular units dissociates into a $(n - 1)$ aggregate plus an uncomplexed monomer. The fact that K_4 is the largest of the four stability constants is corroborated by the experimental observation that a lutetium bisphthalocyanine derivative substituted with only seven crown ether subunits forms only dimeric species and not aggregates under the same conditions.[19] The main driving force for the nonlinear formation of dimers is therefore related to the fourth cation complexation where the two crown-ether subunits are in a correct geometry prior to cation binding.

The intradimer nonlinear effect is however not sufficient to rationalize all our results. In particular, during the titration of [(15C5]$_4$Pc]$_2$Lu with KSCN, dimers should first form before higher molar mass oligomers or polymers could form. If this is the case, the slope of the titration curve would correspond approximately to four cations per two ligands (slope 2/1) whenever the second layer is slightly more difficult to form than the first one. This is by no means observed: high molar mass aggregates form in the very beginning of the titration as demonstrated by the 4:1 slope even for $r < 1$. This is confirmed by the light-scattering measurements. High molar mass aggregates coexist with monomeric species even for small amounts of KSCN. The only way to interpret these results is to postulate, in addition to the previous intradimer nonlinear process, a complementary nonlinear effect: the energy of formation of the second layer must be higher than the energy of formation of the first one (Figure 12).

High molar mass aggregates can coexist with uncomplexed monomeric species if $K'_2 > K'_1$. It is only necessary, for the subsequent layers, to postulate that $K'_n \geq K'_2$ ($n \geq 3$). The equilibrium constant represented by K'_n is related to the energy of formation of the successive stacks. However, since the limiting step for the formation of the complexes corresponds to the binding of the first cation, it seems reasonable to postulate that K'_n is also dominated by the first cation stability constant within a given layer.

The nature of the counterion is essential for the formation of pillarlike aggregates. The picrate and thiocyanate anions both

(18) Lehn, J.-M. *Acc. Chem. Res.* **1978**, *11*, 49.

(19) Pernin, D.; Simon, J. To be published.

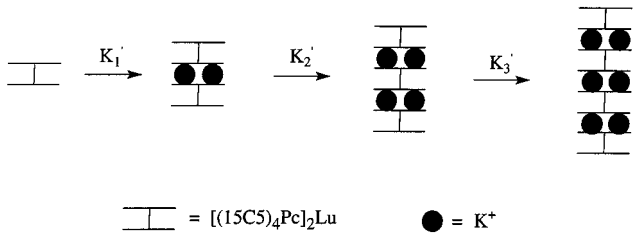

Figure 12. Schematic representation of the nonlinear process effective in the formation of high molar mass aggregates for the first (K_1'), second (K_2') and third (K_3') layer: K_2', K_3', > K_1'.

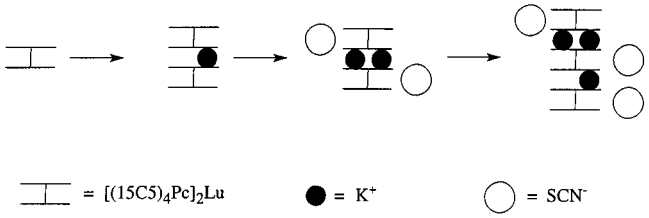

Figure 13. Illustration of the interlayer nonlinear complexation phenomenon. The anions of the ion pairs facilitate the complexation of the first cation of the second layer; this latter can be subsequently filled with potassium ions.

afford high nonlinear effects. Chloride and nitrate potassium salts do not produce any change in the optical spectrum of $[(15C5)_4Pc]_2Lu$. The addition of large excesses of potassium acetate yields only the dimeric form of the lutetium derivative with no detectable amount of aggregates.

On the other hand, the influence of the solvent on the aggregate formation is also important.[20] For the couple $[(15C5)_4Pc]_2Lu/K^+$ picrate in mixtures such as $CHCl_3$/toluene (9:1 or 7:3) the same type of titration curve as those previously shown is observed. However, the addition of more than 20% of methanol in chloroformic solutions leads to a complete disappearance of the aggregates. The titration curve begins to be affected for concentrations of methanol as low as 5%. In 1,4-dichlorobenzene, only dimeric species are detectable.

All these results point out that the nature of the anion and the solvating power of the solvent are important for determining the interlayer nonlinear effects. In chloroformic solutions with a small amount of methanol, strong ion pairs are present in the medium. The presence of the anion in the vicinity of the first dimeric species can facilitate via Coulombic forces the complexation of the first cation of the second layer (Figure 13).

Conclusion

Light-scattering studies have been carried out to elucidate the nature of the aggregates formed when a potassium salt is added to $[(15C5)_4Pc]_2Lu$ chloroformic solutions. Two different theoretical models have been used to interpret the light-scattering results in order to deduce the shape of the aggregates. No definitive conclusion can be given at that stage: either simple rods or rods linked with joints are both in good agreement with the experimental results. X-ray scattering, which permits exploration of a larger domain of q values, could allow us in the near future to draw more definitive conclusions.

The potassium ion-induced aggregation of $[(15C5)_4Pc]_2Lu$ occurs via two successive, positive, highly cooperative effects. This type of behavior is, as far as we know, unique. It is a first step toward the realization of ionoelectronics systems. To continue the lutetium derivative ligands must be functionalized and grafted on a surface.

Experimental Section

The 15-crown-5 substituted derivative **1** was synthesized according to previously reported procedures.[2]

Light-scattering measurements were performed in the "groupe de Physico-Chimie" (ICS-Strasbourg) with a home-built automatized photogoniodiffusometer equipped with a tunable laser[21] (Argon). The working wavelength was 514 nm, so as to minimize light absorption problems due to the lutetium derivative; a vertically polarized light beam was used. The cell was in a bath containing *o*-xylene and the benzene signal was used as a reference. The solutions of $[(15C5)_4Pc]_2Lu$ (10^{-5} M in $CHCl_3$) and KSCN (2×10^{-3} M in MeOH) were filtered through Dynagard 0.2 μm (microgon) filters to remove dust. The potassium salt in MeOH was added portionwise to 8 mL of a chloroformic solution of $[(15C5)_4Pc]_2Lu$. The scattered intensity of light in the θ direction was measured for each ratio $r = [K^+]/[\text{ligand}]$.

A solution 10^{-5} M of $[(15C5)_4Pc]_2Lu$ has been used throughout the experiments. Various amounts of potassium salt (either picrate or SCN^-) were added in order to vary the ratio $r = [K^+]/[(15C5)_4Pc]_2Lu$. Preliminary measurements were carried out with a light-scattering spectrometer FICA at 623.8 nm (He-Ne laser) for the couple K^+ picrate/lutetium complex. An argon laser (514 nm) has been used for studying the titration with KSCN.

Acknowledgment. This work is dedicated to Professor Dr M. Hanack on the occasion of his 65th anniversary. F. Chbab is thanked for having studied the effect of the nature of the solvent on the aggregation processes and P. Bassoul for the drawing shown in Figure 8. J. François is acknowledged for helpful discussions. Mathematica and Lotus applications were used for the calculations. This work is carried out with the help of the European Network contract no. ERBCHRXCT 940558 and the financements provided by CNRS, the city of Paris (ESPCI), and by ULTIMATECH.

JA9644438

(20) Chbab, F.; Toupance, T.; Simon, J. To be published.

(21) Libeyre, R.; Sarazin, D.; François, J. *Polymer B* **1981**, *4*, 53.
(22) Benoit, H.; Hadziioannou, G. *Macromolecules* **1988**, *21*, 1449.
(23) Zimm, B. H. *J. Chem. Phys.* **1948**, *16*, 1093.